



# Non-linear Control of Aerial Manipulator Robots Based on Numerical Methods

David F. Grijalva<sup>(✉)</sup>, Jaime A. Alegría<sup>(✉)</sup>, Víctor H. Andaluz<sup>(✉)</sup>,  
and Cesar Naranjo<sup>(✉)</sup>

Universidad de las Fuerzas Armadas ESPE, Sangolquí, Ecuador  
{dfgrijalva, jaalegría, vhandaluz1, canaranjo}@espe.edu.ec

**Abstract.** This work proposes a kinematic modelling and a non-linear kinematic controller for an autonomous aerial mobile manipulator robot that generates velocity commands for trajectory tracking problem. The kinematic modelling is considered using a hexarotor system and robotic arm. The stability and robustness of the entire control system are tested by this method. Finally, the experiment results are presented and discussed, and validate the proposed controller.

**Keywords:** Aerial manipulator · AMR · Control no lineal

## 1 Introduction

Robotics has greatly evolved and is now present in several areas of the industrial field, as well as the service robotics, where a wide study and research field exists due to its several applications, such as: robotic service assistant in nursing [1]; service robotics with social conscience for guiding and helping passengers in airports [2]; robotics for home assistance [3]; service robot used for preventing collisions [4]. Service robots may present unexpected behaviors that represent economic and safety risks, especially for the human staff around them [5], because of the wide operating field of service robots, some structures have been developed so that they can work in land, water and aerial environments, therefore, they can use wheels, legs, and propellers, as its application requires. For service robotics, one of the main workplaces are locations where there are only flat surfaces for movement, so in order to cover these locations, unmanned aerial vehicles are used (UAV) [6].

Unmanned aerial vehicles, also known as drones, are flying objects that are not manned by a pilot [7]. Aerial vehicles have been under research lately [8] generating several applications, like search and rescue operations, surveillance, handling or grabbing tasks, in which it is needed to include a robotic arm that can limit the vehicle from executing more complex and precise tasks.

The combination of mobile aerial systems with robotic arms is known as aerial mobile manipulators [9], which are a type of unmanned aerial vehicles with the ability to physically interact within an ideally unlimited workspace [6]. The most often used platforms for aerial mobile manipulators are helicopter-type or multicopter with their different varieties: quadrotor, hexarotor or octocopter, combined with robotic arms with

multiple freedom degrees [14]. The main applications of aerial mobile manipulators are: i) *Military field*: transportation of equipment tasks, search under rubble and rescue tasks [11]; ii) *Commercial field*: performing merchandise transportation tasks [10]; iii) *Industrial field*: welding, handling high-rise objects, equipment and light machinery moving, which require high precision for performing the task [9, 10, 12].

The aerial manipulators have recently covered a vast area of research, which has focused its attention on multiple research groups and international companies interested in such technology by boosting robotic systems with manipulation abilities as its main goal [10]; and especially focusing on studying: i) *Construction*: As the complexity of the task or application increases, the advances in mechanical design of the aerial manipulator must innovate and focus on designing channeled fans, boosting tilttable frames mechanisms, and studying the concept of the architecture of a tilttable rotor, which has been a very thoroughly studied topic to increase the flying time of such vehicles [15]; ii) *Energy consumption*: One of the most relevant parameters to be considered in these vehicles is the light weight and the inertia that the robotic arm must present due to the severe limitations of useful load and the convenience to extremely reduce the influence of the arm movement over the UAV's stability, apart from optimizing the tilting angles of the propeller depending on the application [14]; iii) *Modelling*: There are two criteria for modelling an aerial manipulator, which are a) Kinematic analysis, and b) Dynamic analysis. The kinematic analysis determines the movement and restrictions of the mobile manipulator. On the other hand, the dynamic analysis focuses on the study of several pairs and forces intervening in movement (inertia, centrifuge, coriolis, gravity, etc.), focused in using methods and proceedings based in the Newtonian and Lagrangian mechanics. This analysis is crucial for designing and assessing the mechanic structure of the aerial manipulator, as well as sizing the actuators and other parts [13, 15]; iv) *Control*: There are several types of controllers, but they are used depending on the aerial manipulator considerations. Such is the case of the included control that consider the UAV and the robotic arm as a whole system and in these controllers focused in one control-point only, (tip of the robotic arm) are used. There are also controllers focused on not included controllers which are characterized by considering 2 different systems, one for the UAV and one for the robotic arm, and must be applied to the work position, and later the robotic arm controller is used to perform the task [15]. However, it is still necessary to address the technological challenges before the use of this kind of technology can be considered reliable. Among these challenges, the ability to handle impacts during a task of a highly dynamic physical interaction is still an unexplored research topic [9].

This paper presents a non-linear control strategy for resolving the trajectory tracking problem of an Aerial manipulator robot that will be defined with the acronym ARM. Which is constituted by an hexacopter mounting a robotic arm of 3 degrees of freedom mounted on back of base. For the design of the controller, the kinematic model of the AMR is used which has as input the velocity and orientation, this controller is designed based on nine velocities commands of the AMR, six corresponding to the aerial platform: forward, lateral, up/downward and orientation, the last three are those who command the manipulator robot. It is also pointed out that the workspace has a single reference that is located in the operative end of the AMR  $R(x\ y\ z)$ . The stability of the controller

is analyzed by the Lyapunov's method and to validate the proposed control algorithm, experimental processes are presented and discussed in this paper.

The document is organized as described below. Section 1 describes the characteristics and applications of the aerial manipulators. Section 2 includes the movement characteristics of the hexarotor. Section 3 describes its kinematic model. Section 4 details the control to be implemented in the aerial manipulator, stability and robustness analysis. Section 5 includes the results obtained from the experimental tests. And, Sect. 6 presents the conclusions.

## 2 Motion Characteristics

An UAV is an unmanned aerial vehicle, which when combined with a robotic arm turns into an aerial manipulator, Fig. 1 shows the combination of a rotational-frames vehicle with an anthropomorphic-type robotic arm.

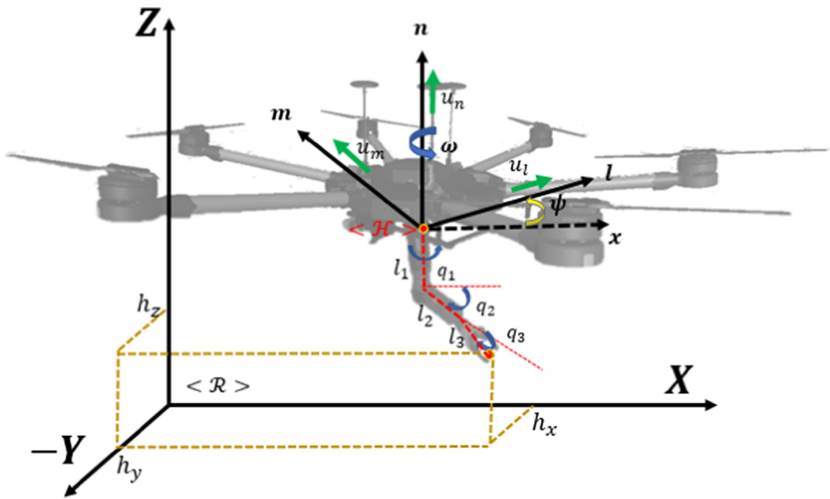


Fig. 1. Structure of hexarotor and its frames

Since this work is formed by a 3-DOF robotic arm on an hexarotor UAV, as shown in Fig. 1, in which the two principal forces for moving it are gravity and the rotors thrust, its movements are controlled by several effects, whether mechanical or aerodynamic. The main effects on the hexarotor are listed in Table 1.

## 3 AMR Model

The aerial manipulator robot configuration is defined by a vector  $\mathbf{q} = [\mathbf{q}_h^T \mathbf{q}_a^T]^T$  where  $\mathbf{q}_h = [x_u \ y_u \ z_u \ \psi]^T$  that represents the specific coordinates of the UAV, and  $\mathbf{q}_a = [q_1 \ q_2 \ q_3]^T$  the specific coordinates of the robotic arm.

**Table 1.** The main effects on the acting hexarotor

Effects	Fountainhead
Aerodynamics effects	Rotating propellers
Inertiel counter torque	Velocity change of propellers
Effect of gravity	Position of the center of mass
Gyroscopic effects	Change in the direction of the drone
Friction effect	All drone movements

Where, the next system of equations represents the direct kinematic model of the ARM:

$$\begin{cases} h_x = x_u + l_2 \cos(q_1 + \psi) \cos(q_2) + l_3 \cos(q_1 + \psi) \cos(q_2 + q_3) \\ h_y = y_u + l_2 \sin(q_1 + \psi) \cos(q_2) + l_3 \sin(q_1 + \psi) \cos(q_2 + q_3) \\ h_z = z_u + l_1 + l_2 \sin(q_2) + l_3 \sin(q_2 + q_3) \end{cases} \quad (1)$$

The instantaneous kinematic model of an AMR gives the derivative of its end-effector location as a function of the derivatives of both the robotic arm configuration and the location of the UAV, it is worth emphasizing that it is practically the partial derivative of Eq. (1).

$$\dot{\mathbf{h}}(t) = \frac{df}{d\mathbf{q}}(\mathbf{q})\mathbf{v}(t)$$

where,  $\dot{\mathbf{h}}(t) = [\dot{h}_x \ \dot{h}_y \ \dot{h}_z]^T$  is the vector of the end-effector velocity,  $\mathbf{v}(t) = [u_l \ u_m \ u_n \ \omega \ \dot{q}_1 \ \dot{q}_2 \ \dot{q}_3]^T$  is the control vector of mobility of the AMR.

Now, after replacing  $\mathbf{J}(\mathbf{q}) = \frac{df}{d\mathbf{q}}(\mathbf{q})\mathbf{v}(t)$  in the above equation, we obtain

$$\dot{\mathbf{h}}(t) = \mathbf{J}(\mathbf{q})\mathbf{v}(t) \quad (2)$$

where,  $\mathbf{J}(\mathbf{q}) \in \mathbb{R}^{3 \times 7}$  is the Jacobian matrix that defines a linear mapping between the vector of the AMR velocities  $\mathbf{v}(t) \in \mathbb{R}^7$  and the vector of the end-effector velocity  $\dot{\mathbf{h}}(t) \in \mathbb{R}^3$ .

## 4 Control Algorithm: Numerical Methods

Through Euler's approximation to the kinematic model for AMR trajectory tracking, the following discrete kinematic model is obtained.

$$\mathbf{h}(k+1) = \mathbf{h}(k) + T_0 \mathbf{J}(\mathbf{q}(k)) \mathbf{v}_{ref}(k) \quad (3)$$

where, values of  $\mathbf{h}$  at the discrete time  $t = kT_0$  will be denoted as  $\mathbf{h}(k)$ ,  $T_0$  is the sample time, and  $k \in \{1, 2, 3, 4, 5, \dots\}$ . Next by the Markov property and to adjusting the performance of the proposed control law, the states vector  $\mathbf{h}(k+1)$  is replaced by,

$$\mathbf{h}(k+1) = \mathbf{h}_d(k+1) - \mathbf{W}(\mathbf{h}_d(k) - \mathbf{h}(k)) \quad (4)$$

where,  $\mathbf{W}$  is weight matrix of control errors defined by  $\mathbf{h}_d(k) - \mathbf{h}(k)$ .

For the design of the control law is used the Euler's approximation of the kinematic model of the ARM (2) and in turn the property of Markov (3), hence

$$\begin{aligned} \mathbf{h}_d(k+1) - \mathbf{W}(\mathbf{h}_d(k) - \mathbf{h}(k)) &= \mathbf{h}(k) + T_0 \mathbf{J}(\mathbf{q}(k)) \mathbf{v}_{ref}(k) \\ \mathbf{J}(\mathbf{q}(k)) \mathbf{v}_{ref}(k) &= \frac{1}{T_0} (\mathbf{h}_d(k+1) - \mathbf{W}(\mathbf{h}_d(k) - \mathbf{h}(k))) \end{aligned} \quad (5)$$

Equation (4) can be represented by,  $\mathbf{J}\mathbf{v} = \mathbf{b}$ , through the properties of Linear Algebra the following control law is proposed for trajectory tracking

$$\mathbf{v}_{ref} = \mathbf{J}^\# \mathbf{b}$$

where  $\mathbf{J}^\#(\mathbf{q}(k)) = \mathbf{J}^T(\mathbf{q}(k))(\mathbf{J}(\mathbf{q}(k))\mathbf{J}^T(\mathbf{q}(k)))^{-1}$  represents the pseudoinverse matrix of  $\mathbf{J}(\delta(k), \mathbf{q}(k))$ , hence, the proposed control law is:

$$\mathbf{v}_{ref}(k) = \frac{1}{T_0} \mathbf{J}^\#(\mathbf{q}(k)) (\mathbf{h}_d(k+1) - \mathbf{W}(\mathbf{h}_d(k) - \mathbf{h}(k)) - \mathbf{h}(k)) \quad (6)$$

where  $\mathbf{v}_{ref}(k) = \begin{bmatrix} u_{l_{ref}}(k) & u_{m_{ref}}(k) & u_{n_{ref}}(k) & \omega_{r_{ref}}(k) & \dot{q}_{1_{ref}}(k) & \dot{q}_{2_{ref}}(k) & \dot{q}_{3_{ref}}(k) \end{bmatrix}^T$  is the maneuverability vector of AMR.

#### 4.1 Stability Análisis

In order to evaluate the behavior of the AMR control errors, the stability analysis is performed, for which it is considered perfect velocity tracking, *i.e.*  $\mathbf{v}_{ref}(k) \equiv \mathbf{v}(k)$ . The behavior of control errors can be obtained by relating the dictated model of the AMR (3) and the proposed control law (6)

$$\frac{1}{T_0} (\mathbf{h}(k+1) - \mathbf{h}(k)) = \frac{1}{T_0} \mathbf{J}\mathbf{J}^\# (\mathbf{h}_d(k+1) - \mathbf{W}(\mathbf{h}_d(k) - \mathbf{h}(k)) - \mathbf{h}(k)).$$

Where  $\mathbf{I} = \mathbf{J}\mathbf{J}^\#$  simplifying the terms, the closed-loop equation is

$$\mathbf{h}_d(k+1) - \mathbf{h}(k+1) = \mathbf{W}(\mathbf{h}_d(k) - \mathbf{h}(k)) \quad (7)$$

where the control error is defined by  $\tilde{\mathbf{h}}(k) = \mathbf{h}_d(k) - \mathbf{h}(k)$  and  $\tilde{\mathbf{h}}(k+1) = \mathbf{h}_d(k+1) - \mathbf{h}(k+1)$ , therefore (7) can be rewritten as

$$\tilde{\mathbf{h}}(k+1) = \mathbf{W}\tilde{\mathbf{h}}(k). \quad (8)$$

In order to evaluate the evolution of the control error, the *i*-th control error is considered,  $\tilde{h}_i(k+1)$  and  $\tilde{h}_i(k)$  the weight matrix is defined as  $\mathbf{W} = \text{diag}(w_{11}, w_{22}, w_{33})$

$$\tilde{h}_i(k+1) = w_{ii}\tilde{h}_i(k) \quad (9)$$

Table 2 represents the evolution of the *i*-th control error for different instants of time

If  $k \rightarrow \infty$  then  $\tilde{h}_i(\infty) = w_{ii}^\infty \tilde{h}_i(1)$ , therefore so that the  $\tilde{h}_i(\infty) \rightarrow 0$  values of the diagonal weight matrix must be between  $0 < \text{diag}(w_{11}, w_{22}, w_{33}) < 1$ . As described, it can be concluded that control errors have asymptotic stability, that is to say  $\tilde{h}_i(k) \rightarrow 0$ , when  $k \rightarrow \infty$ .

**Table 2.** Evolution of *it-th* control error.

$k$	$\tilde{h}_i(k+1)$	$w_{ii}\tilde{h}_i(k)$
1	$\tilde{h}_i(2)$	$w_{ii}\tilde{h}_i(1)$
2	$\tilde{h}_i(3)$	$w_{ii}\tilde{h}_i(2) = w_{ii}^2\tilde{h}_i(1)$
3	$\tilde{h}_i(4)$	$w_{ii}^3\tilde{h}_i(1)$
$\vdots$	$\vdots$	$\vdots$
$n$	$\tilde{h}_i(n+1)$	$w_{ii}^n\tilde{h}_i(1)$

## 4.2 Robustness Analysis

In order to the robustness analysis it is considered:

$$\mathbf{v}(k) = \mathbf{v}_{ref}(k) - \tilde{\mathbf{v}}(k)$$

The behavior of control errors can be obtained by relating the dictated model of the AMR (3), the proposed control law (6)

$$\frac{1}{T_0}(\mathbf{h}(k+1) - \mathbf{h}(k)) = \frac{1}{T_0}\mathbf{J}\mathbf{J}^\#(\mathbf{h}_d(k+1) - \mathbf{h}(k) - \mathbf{W}(\tilde{\mathbf{h}}(k)) - \mathbf{J}\tilde{\mathbf{v}}(k))$$

where  $\mathbf{I} = \mathbf{J}\mathbf{J}^\#$  simplifying the terms, the equation is

$$\begin{aligned} \mathbf{J}\tilde{\mathbf{v}}(k) &= \mathbf{h}_d(k+1) - \mathbf{h}(k+1) - \mathbf{W}(\tilde{\mathbf{h}}(k)) \\ \tilde{\mathbf{h}}(k+1) &= \mathbf{W}(\tilde{\mathbf{h}}(k)) + \mathbf{J}\tilde{\mathbf{v}}(k) \\ \tilde{\mathbf{h}}(n+1) &= \mathbf{W}^n(\tilde{\mathbf{h}}(n)) + \mathbf{J}\tilde{\mathbf{v}}(n) \end{aligned} \quad (10)$$

if  $0 < \mathbf{W} < 1$  and  $n \rightarrow \infty$

$$\therefore \|\tilde{\mathbf{h}}(n+1)\| < \|\mathbf{J}\tilde{\mathbf{v}}(n)\|.$$

## 5 Experimental Results

The experimental tests of the proposed control algorithm are performed on the Aerial Manipulator Robot consisting of a 3DOF robotic arm, a UAV (Matrice 600 pro) and the PC where the control actions are sent. Figure 2 shows the ARM used for the experimental tests.

A desired trajectory is established to verify the performance of the proposed control law. For the compliance of the trajectory the AMR PC sends the control actions that allow the AMR mobility and the tracking of the trajectory. It is necessary to know the initial conditions for the execution of the control law. The initial conditions are defined



**Fig. 2.** Aerial manipulator robot

by:  $x_{UAV}(1)$ ,  $y_{UAV}(1)$ ,  $z_{UAV}(1)$ ,  $q_1(1)$ ,  $q_2(1)$ ,  $q_3(1)$ . The conditions can be defined from the controller or read the actual positions of the robotic arm and drone. Table 3 below shows the initial conditions and the desired values of the trajectory.

Figure 3, shows the desired and realized trajectory of the final effector. It can be seen that the proposed controller has a good performance. The data of the trajectory made are real obtaining experimental tests.

The control errors are close to zero as shown in Fig. 4. This allows to say that the controller has a good performance, due to the fact that in the experimental tests in spite of the existence of perturbations the AMR fulfills the established trajectory.

The maneuverability commands shown in Fig. 5 are those that allow the movement of the UAV defined by  $u_l$  movement forward,  $u_m$  lateral move,  $u_n$  up and down motion and  $\psi$  orientation of UAV.

**Table 3.** Initial conditions and target trajectory values

Variables	Values	Variables	Values
$x_{UAV}(1)$	0 [m]	$q_3(1)$	0.4 [rad]
$y_{UAV}(1)$	0 [m]	$h_{xd}(t)$	$5 \cos(0.05t) + 5$ [m]
$z_{UAV}(1)$	0 [m]	$h_{yd}(t)$	$5 \sin(0.05t) + 5$ [m]
$\psi_{UAV}(1)$	0 [m]	$h_{zd}(t)$	$\sin(0.3t) + 16$ [m]
$q_1(1)$	0.2 [rad]	$\psi_{zd}(t)$	$\tan^{-1}(\dot{h}_{yd} / \dot{h}_{xd})$ [rad]
$q_2(1)$	0.8 [rad]		

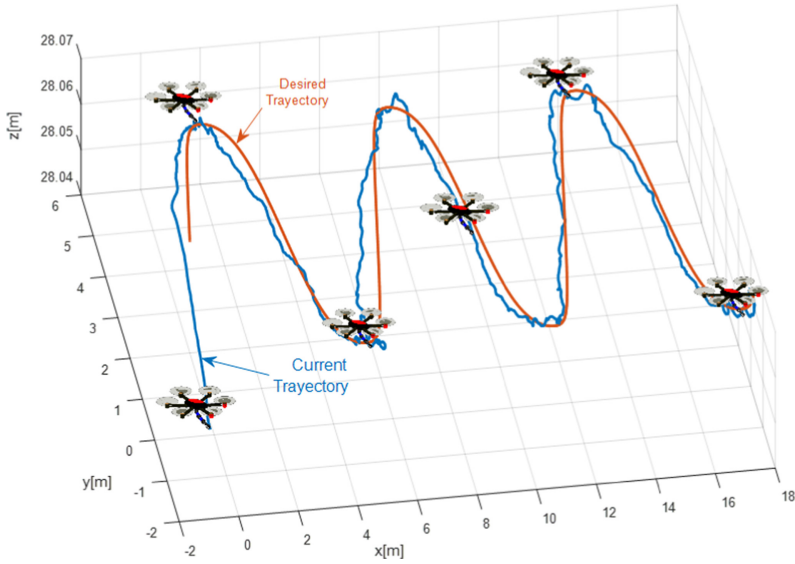


**Fig. 3.** Stroboscopic movement of the aerial manipulator robot in the trajectory tracking problem.

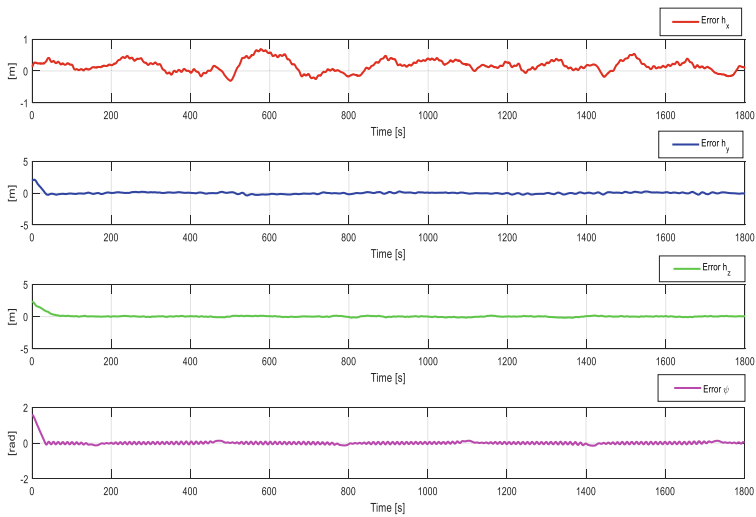


**Fig. 4.** Control errors of the end-effector of the aerial manipulator robot.

The robotic arm maneuverability commands are defined by  $q_1$ ,  $q_2$  y  $q_3$  which will allow the end effector to comply with the established trajectory (Fig. 6).



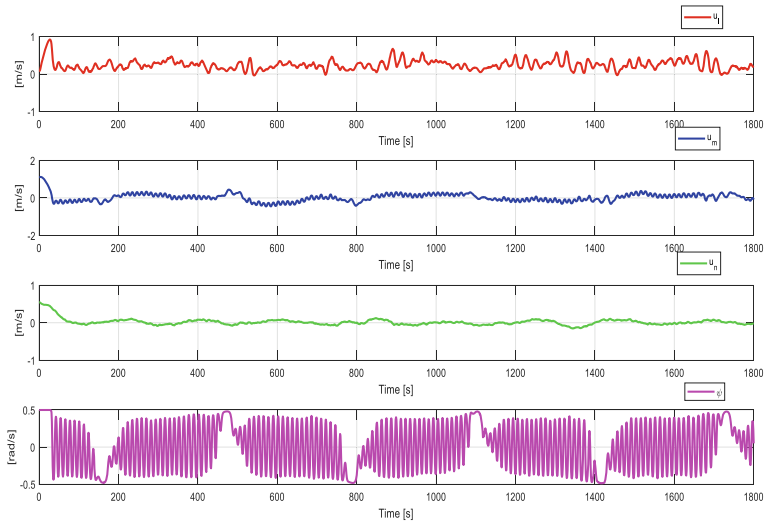


**Fig. 5.** Commands of maneuverability of aerial manipulator robot

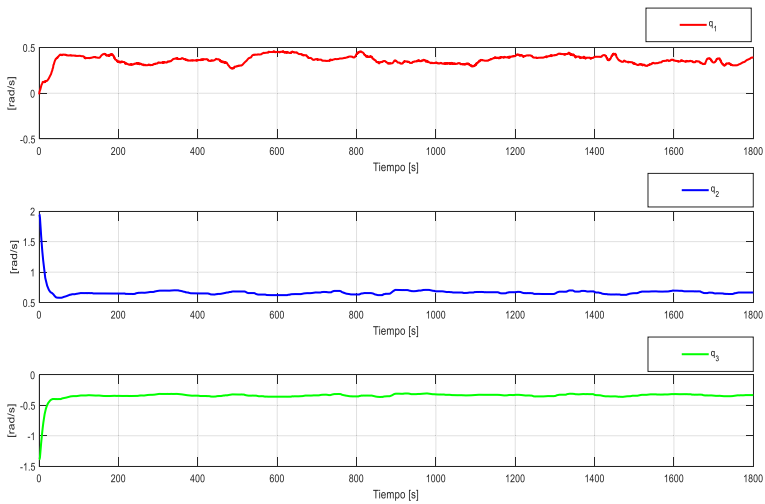


**Fig. 6.** Commands of maneuverability of Arm.

## 6 Conclusions

In this article, a non-linear controller based on numerical methods for trajectory tracking was proposed, through the kinematic analysis that allowed the implementation of an precise model of an aerial manipulator robot, the same one that was used for experimental tests. The easy implementation of the controller and its simplicity make it much more understandable and easy to use, in addition to presenting excellent stability and robustness, in analytical tests and experimental tests. The results of the experimental tests

have demonstrated the capacity of the controller to perform control actions globally and asymptotically.

**Acknowledgements.** The authors would like to thank the Corporación Ecuatoriana para el Desarrollo de la Investigación and Academia CEDIA for the financing given to research, development, and innovation, through the CEPRA projects, especially the project CEPRA-XIII-2019-08; Sistema colaborativo de robots aéreos para manejar cargas con un consumo óptimo de recursos; also to Universidad de las Fuerzas Armadas ESPE, Escuela Superior Politécnica de Chimborazo, Universidad Nacional de Chimborazo, Universidad tecnológica Indoamérica, Universidad internacional de Ecuador, Universidad central de Venezuela, and Grupo de Investigación ARSI, for the support to develop this work.

## References

1. Baumgarten, S., Jacobs, T., Graf, B.: The robotic service assistant-relieving the nursing staff of workload. In: 50th International Symposium on Robotics, ISR 2018, pp. 1–4. VDE, June 2018
2. Triebel, R., et al.: SPENCER: a socially aware service robot for passenger guidance and help in busy airports. In: Wettergreen, D.S., Barfoot, T.D. (eds.) *Field and Service Robotics*. STAR, vol. 113, pp. 607–622. Springer, Cham (2016). [https://doi.org/10.1007/978-3-319-27702-8\\_40](https://doi.org/10.1007/978-3-319-27702-8_40)
3. Cesta, A., Cortellessa, G., Orlandini, A., Sorrentino, A., Umbrico, A.: A semantic representation of sensor data to promote proactivity in home assistive robotics. In: Arai, K., Kapoor, S., Bhatia, R. (eds.) *IntelliSys 2018*. AISC, vol. 868, pp. 750–769. Springer, Cham (2019). [https://doi.org/10.1007/978-3-030-01054-6\\_53](https://doi.org/10.1007/978-3-030-01054-6_53)
4. Mendes, M., Coimbra, A.P., Crisóstomo, M.M., Cruz, M.: Vision-based collision avoidance for service robot. In: Ao, S.-I., Gelman, L., Kim, H.K. (eds.) *WCE 2017*, pp. 233–248. Springer, Singapore (2019). [https://doi.org/10.1007/978-981-13-0746-1\\_18](https://doi.org/10.1007/978-981-13-0746-1_18)
5. Guerrero-Higueras, Á.M., Rodríguez-Lera, F.J., Martín-Rico, F., Balsa-Comerón, J., Matellán-Olivera, V.: Accountability in mobile service robots. In: Fuentetaja Pizán, R., García Olaya, Á., Sesmero Lorente, M.P., Iglesias Martínez, J.A., Ledezma Espino, A. (eds.) *WAF 2018*. AISC, vol. 855, pp. 242–254. Springer, Cham (2019). [https://doi.org/10.1007/978-3-319-99885-5\\_17](https://doi.org/10.1007/978-3-319-99885-5_17)
6. Ortiz, J.S., et al.: Modeling and kinematic nonlinear control of aerial mobile manipulators. In: Zeghloul, S., Romdhane, L., Laribi, M.A. (eds.) *Computational Kinematics*. MMS, vol. 50, pp. 87–95. Springer, Cham (2018). [https://doi.org/10.1007/978-3-319-60867-9\\_11](https://doi.org/10.1007/978-3-319-60867-9_11)
7. Varela-Aldás, J., Andaluz, V.H., Chicaiza, F.A.: Modelling and control of a mobile manipulator for trajectory tracking. In: 2018 International Conference on Information Systems and Computer Science. INCISCOS, pp. 69–74. IEEE, November 2018
8. Škorput, P., Mandžuka, S., Gregurić, M., Vrančić, M.T.: Applying unmanned aerial vehicles (UAV) in traffic investigation process. In: Karabegović, I. (ed.) *NT 2019*. LNNS, vol. 76, pp. 401–405. Springer, Cham (2020). [https://doi.org/10.1007/978-3-030-18072-0\\_46](https://doi.org/10.1007/978-3-030-18072-0_46)
9. Bartelds, T., Capra, A., Hamaza, S., Stramigioli, S., Fumagalli, M.: Compliant aerial manipulators: toward a new generation of aerial robotic workers. *IEEE Robot. Autom. Lett.* **1**(1), 477–483 (2016)
10. Andaluz, V.H., Carvajal, C.P., Pérez, J.A., Proaño, L.E.: Kinematic nonlinear control of aerial mobile manipulators. In: Huang, Y., Wu, H., Liu, H., Yin, Z. (eds.) *ICIRA 2017*. LNCS (LNAI), vol. 10464, pp. 740–749. Springer, Cham (2017). [https://doi.org/10.1007/978-3-319-65298-6\\_66](https://doi.org/10.1007/978-3-319-65298-6_66)

11. Suárez, A., Sanchez-Cuevas, P., Fernandez, M., Perez, M., Heredia, G., Ollero, A.: Lightweight and compliant long reach aerial manipulator for inspection operations. In: 2018 IEEE/RSJ International Conference on Intelligent Robots and Systems (IROS), pp. 6746–6752. IEEE, October 2018
12. Tognon, M., Franchi, A.: Dynamics, control, and estimation for aerial robots tethered by cables or bars. *IEEE Trans. Robot.* **33**(4), 834–845 (2017)
13. Molina, M.F., Ortiz, J.S.: Coordinated and cooperative control of heterogeneous mobile manipulators. In: Ge, S.S., et al. (eds.) ICSR 2018. LNCS (LNAI), vol. 11357, pp. 483–492. Springer, Cham (2018). [https://doi.org/10.1007/978-3-030-05204-1\\_47](https://doi.org/10.1007/978-3-030-05204-1_47)
14. Andaluz, V.H., et al.: Nonlinear controller of quadcopters for agricultural monitoring. In: Bebis, G., Boyle, R., Parvin, B., Koracin, D., et al. (eds.) ISVC 2015. LNCS, vol. 9474, pp. 476–487. Springer, Cham (2015). [https://doi.org/10.1007/978-3-319-27857-5\\_43](https://doi.org/10.1007/978-3-319-27857-5_43)
15. Rajappa, S., Ryll, M., Bühlhoff, H.H., Franchi, A.: Modeling, control and design optimization for a fully-actuated hexarotor aerial vehicle with tilted propellers. In: 2015 IEEE International Conference on Robotics and Automation (ICRA), pp. 4006–4013. IEEE, May 2015